

## Study of muon bundles generated by UHE cosmic rays at large zenith angles

I.I. Yashin<sup>a</sup>, M.B. Amelchakov<sup>a</sup>, N.S. Barbashina<sup>a</sup>, A.G. Bogdanov<sup>a</sup>, D.V. Chernov<sup>a</sup>,  
D.M. Gromushkin<sup>a</sup>, V.V. Kindin<sup>a</sup>, R.P. Kokoulin<sup>a</sup>, K.G. Kompaniets<sup>a</sup>, G. Mannocchi<sup>b</sup>,  
O.S. Matveeva<sup>a</sup>, A.A. Petrukhin<sup>a</sup>, D.A. Room<sup>a</sup>, O. Saavedra<sup>c</sup>, V.V. Shutenko<sup>a</sup>,  
D.A. Timashkov<sup>a</sup> and G. Trincherò<sup>b</sup>

(a) *Moscow Engineering Physics Institute, Kashirskoe shosse, 31, Moscow 115409, Russia*

(b) *Istituto di Fisica dello Spazio Interplanetario del CNR, Sezione di Torino, Torino 10133, Italy*

(c) *Dipartimento di Fisica Generale dell'Università di Torino, Torino 10125, Italy*

Presenter: I.I. Yashin (yashin@nevod.mephi.ru), rus-yashin-II-abs1-he13-oral

The first data on a new EAS observable – local muon density spectra measured in a wide range of zenith angles by means of a large-area coordinate detector DECOR are presented. Comparison with CORSIKA-based simulation results is discussed.

### 1. Introduction

Muon bundles, or groups of muons with close quasi-parallel tracks, detected at the Earth's surface at large zenith angles ( $60^\circ - 90^\circ$ ) are a useful tool to obtain additional information on primary cosmic-ray spectrum, composition and characteristics of hadron-nucleus interaction at high energies. Due to the properties of the atmosphere, the observation depth and the distance to the generation level rapidly vary with the zenith angle increase; therefore, investigations of local muon density spectra at different zenith angles allow to study the primary flux in a wide range of energies by means of a single detector with large area and high angular resolution. For these purposes, the coordinate detector DECOR [1] was constructed in frame of the joint Russian-Italian project. DECOR represents a modular multi-layer system of plastic streamer tube chambers, arranged in the building of experimental complex NEVOD [2] around the Cherenkov water calorimeter with volume  $2000 \text{ m}^3$ . The side part of DECOR includes eight vertical 8-layer assemblies (supermodules, SM) of chambers with the total area  $70 \text{ m}^2$ . Selection of events by the triggering system is based on coincidences between the signals from different SM and signals formed by the system of Cherenkov detector. A more detailed description of the experimental complex is given in [3]. Preliminary analysis of the data obtained with the NEVOD-DECOR complex demonstrated the ability of such not very large detector to perform cosmic ray investigations in a wide energy range from  $10^{14}$  eV (for low multiplicity bundles) to more than  $10^{17}$  eV (bundles of large multiplicities at large zenith angles) by means of EAS muon component observation.

### 2. Experimental data

Experimental data collected during long-term 2002-2004 experimental runs (10579 hr live time) are used. Procedure of muon bundle selection includes several stages. On a trigger level, the events with a coincidence of signals from any three SM of the side part of DECOR are recorded. At the second stage, a program selection of muon bundle candidates is performed; events with at least 3 reconstructed tracks parallel within  $5^\circ$ -cone are retained. Then, the candidates are visually scanned independently by two experts with a help of computer-aided graphic interface; the events are finally classified and muon tracks are counted. After cross-comparison of the experts' results, event lists containing muon bundle multiplicity, estimates of zenith and azimuth angles and some auxiliary information are formed. As a rule, muon bundle events have a bright signature in the coordinate detector, and are unambiguously selected.

At large zenith angles ( $\theta \geq 60^\circ$ ), multi-particle events with parallel tracks are formed almost by muons only; however, this is not the case for lower zenith angles. Therefore, for  $\theta < 60^\circ$  only the events in two limited sectors of azimuth angle (with six SMs shielded by the NEVOD water tank, threshold muon energy about 1 GeV) were selected. The experimental statistics analysed for the moment for several zenith angle intervals and minimal muon multiplicities are summarised in Table 1. Among the selected events, there are bundles with zenith angles up to  $87^\circ$ , and with multiplicity more than 100 parallel tracks.

**Table 1.** Experimental statistics

Muon multiplicity	Zenith angle range	Live time, hr	Number of events
$\geq 3$	$30 - 40^\circ$	250.5	2258
$\geq 3$	$40 - 60^\circ$	250.5	3748
$\geq 5$	$\geq 60^\circ$	630.0	3033
$\geq 10$	$\geq 75^\circ$	10579	208

### 3. Local muon density spectrum

The approach to the analysis of the data is based on the following steps: deconvolution of measured muon bundle distributions to detector-independent spectra of events in local muon density; convolution of muon lateral distribution functions (LDF) calculated by means of the CORSIKA code with certain primary spectrum/composition models; comparison of experimental and calculated muon density spectra.

Observed muon bundle multiplicity  $m$  is related to the local muon density  $D$  (measured in particles/m<sup>2</sup>) as  $\langle m \rangle \sim S_{eff} D$ . The detector effective area  $S_{eff}$  depends on the shower arrival direction and varies from 20 m<sup>2</sup> to 45 m<sup>2</sup>. Deconvolution of the observed muon bundle distributions in multiplicity, zenith and azimuth angles  $N_{\mu}(m, \theta, \varphi)$  to the local muon density spectra  $dF/dD$  for several angular intervals was carried out taking into account the dependence of  $S_{eff}$  on the angles, Poissonian fluctuations of the number of particles that hit the detector, and trigger conditions. As a first iteration for the deconvolution procedure, a following semi-empirical fit was used:

$$dF/dD \sim D^{-(\beta+1)} \cdot \cos^\alpha \theta. \quad (1)$$

Without considering shower fluctuations, the integral spectrum of EAS events as function of local muon density  $F(D)$  (measured in sr<sup>-1</sup> s<sup>-1</sup>) is determined by the primary spectrum  $dN/dE$  and muon LDF  $\rho(E, r)$ :

$$F(\geq D) = \int_0^\infty 2\pi r dr \int_{E_{min}(r, D)}^\infty (dN/dE) \cdot dE, \quad (2)$$

where  $E_{min}$  is defined by the solution of the equation  $\rho(E, r) = D$ . Here  $r$  is the distance between the shower axis and the point of detector location. The differential local density spectrum  $dF/dD$  may be easily obtained as derivative of Eq. (2). Muon LDFs in a plane orthogonal to the shower axis were calculated on the basis of CORSIKA code [4] (version 6.200) for zenith angles  $35^\circ$ ,  $50^\circ$ ,  $70^\circ$  and  $80^\circ$ , different primaries (protons and iron nuclei), a set of fixed primary energies, and two combinations of hadron interaction models: QGSJET01c+GHEISHA2002 and SIBYLL2.1 + FLUKA2003.1b. To find the integration limit over the energy in calculations of (2), a linear interpolation in  $(\log E, \log \rho)$ -variables was applied.

As a model of the primary flux, a power type all-particle differential spectrum in the form  $dN/dE = 5.0 \times (E, \text{GeV})^{-2.7} \text{ cm}^{-2} \text{ s}^{-1} \text{ sr}^{-1} \text{ GeV}^{-1}$  below the knee energy, steepening to  $(\gamma + 1) = 3.1$  above the knee (4 PeV) was used. This spectrum is close to MSU spectrum as given in [5], it is not very much different from the Akeno data around the knee, and is in a reasonable agreement with Fly's Eye "stereo" results around  $10^{18}$  eV. The region accessible to the present study is limited at low energies by about  $10^{15}$  eV because of low muon densities in such EAS. On the other hand, for events with  $D > 1$  muons/m<sup>2</sup> at angles around  $80^\circ$  there are

statistical limitations (about 10 such events detected). Estimations show that the upper limit of effective energies corresponds to about  $10^{18}$  eV.

#### 4. Discussion

Differential local muon density spectra for zenith angles  $35^\circ$ ,  $50^\circ$ ,  $70^\circ$ , and  $80^\circ$  are presented in Fig. 1. For the convenience of representation, data are multiplied by  $D^3$ . The points in the figure are obtained from 4 different sub-sets of experimental data (see Table 1); only statistical errors are shown. Horizontal error bars illustrate the rms-spread of muon densities contributing to events with a given average density. The curves are calculation results for two combinations of hadronic interaction models and two extreme versions of primary composition (only protons and only iron). At moderate zenith angles, a reasonable agreement of preliminary DECOR results with CORSIKA-based simulation is observed. However, for  $80^\circ$  experimental points are below calculations by about a factor of 2.

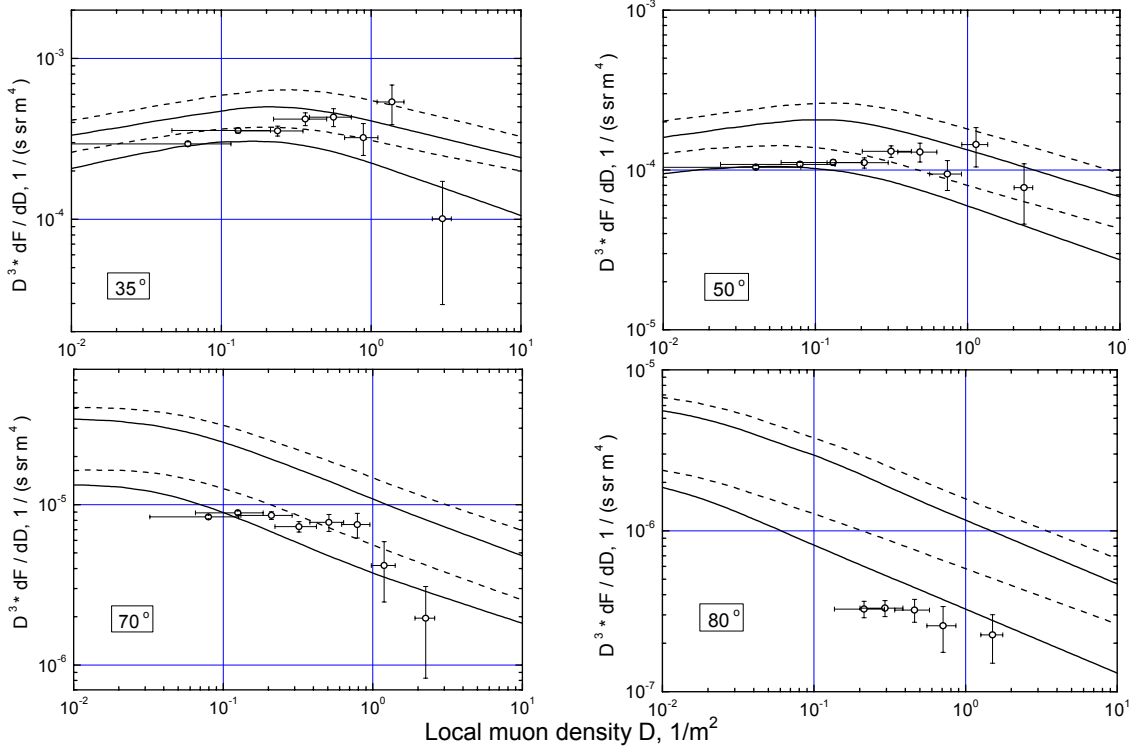


**Figure 1.** Differential spectra of local muon density for different zenith angles. Points represent the experimental data; curves are calculation results (dashed and solid curves correspond to QGSJET and SIBYLL models, respectively; upper curves are for iron primaries and lower ones for protons).

In Fig.2, zenith angular distribution for local muon density exceeding a fixed threshold ( $D > 0.2$  muons/m<sup>2</sup>) is shown. The dashed line represents a fit of experimental data in the form of a power function of zenith angle cosine. CORSIKA-based calculations (the curves) exhibit a slower decrease of the intensity with the increase of zenith angle. In principle, such deviation could be explained by a steeper primary spectrum than that assumed in the calculations. However, such supposition unlikely is compatible with the data since the measured spectra favor somewhat lower spectrum slope than calculations at all zenith angles (see Fig.1). Table 2 represents the results of the fits of different sub-sets of experimental data (for different multiplicity and zenith angle ranges) in form of Eq.(1). As it is seen from the table, the slope of muon density spectrum

increases with the increase of multiplicity and of zenith angle (and, consequently, with the increase of the primary energy). Such behavior does not contradict a usual picture of a steepening primary spectrum.

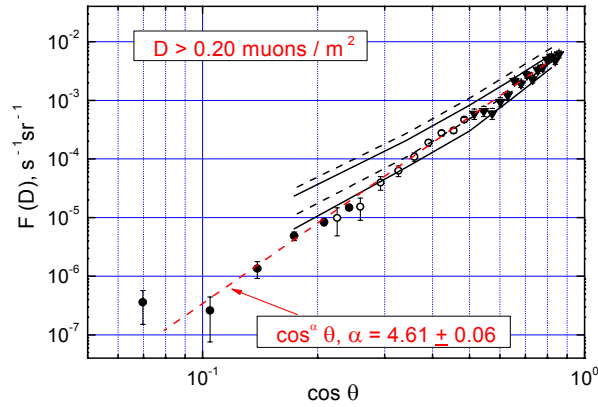


**Figure 2.** Zenith angle dependence of the integral intensity for the local muon density  $D > 0.2$  muons/m<sup>2</sup>. Points correspond to different sub-sets of DECOR data; curves are calculation results (notations are the same as in Figure 1).

**Table 2.** Estimation of parameters of local muon density distribution.

Multiplicity	Zenith angle range	$\beta$	$\alpha$
$\geq 3$	$30 - 40^\circ$	$1.865 \pm 0.024$	$4.01 \pm 0.60$
$\geq 3$	$40 - 60^\circ$	$1.945 \pm 0.018$	$4.50 \pm 0.12$
$\geq 5$	$\geq 60^\circ$	$2.087 \pm 0.030$	$4.42 \pm 0.09$
$\geq 10$	$\geq 75^\circ$	$2.144 \pm 0.134$	$4.15 \pm 0.35$

## 5. Conclusions

The local muon density spectra in a wide range of zenith angles ( $30^\circ - 80^\circ$ ), corresponding to primary particle energies in the interval  $10^{15} - 10^{18}$  eV, have been measured for the first time. The slope of muon density spectrum increases with effective primary energy. At moderate zenith angles, a reasonable agreement with CORSIKA-based simulations (in frame of conservative suppositions on all-particle primary spectrum) is found. However, at large zenith angles a significant deviation from CORSIKA predictions appears; simulation results do not reproduce the measured angular dependence of the event intensity. The reasons of these deviations may be different: deficiencies in hadron interaction description in the forward region; problems related with shower development and muon propagation in thick atmosphere at large zenith angles; methodical reasons caused by insufficient understanding of selection and reconstruction efficiency, etc. Therefore, a thorough analysis both of experimental procedure and of calculation results is necessary.

## 6. Acknowledgements

The research is performed at the Complex NEVOD (reg. no. 01-63) with the support of the Ministry of Education and Science and Federal Agency for Science and Innovations of the Russian Federation.

## References

- [1] M.B. Amelchakov et al., Proc. 27th ICRC, Hamburg, 3, 1267 (2001).
- [2] V.M. Aynutdinov et al., Astrophysics and Space Science, 258, 105 (1998).
- [3] I.I. Yashin et al., Proc. 28th ICRC, Tsukuba, 3, 1147 (2003).
- [4] D. Heck et al., FZK Report, FZKA 6019 (1998).
- [5] S. Eidelman et al. (Particle Data Group), Phys. Lett. B, 592, 1 (2004).